ISSN 1029-9599, Physical Mesomechanics, 2022, Vol. 25, No. 4, pp. 296–305. © Pleiades Publishing, Ltd., 2022.
Russian Text © The Author(s), 2022, published in Fizicheskaya Mezomekhanika, 2022, Vol. 25, No. 2, pp. 24–34.

Reverse Engineering of Mechanical and Tribological Properties of Coatings: Results of Machine Learning Algorithms

D. M. Pashkov[1,2], O. A. Belyak[1], A. A. Guda[1,2]*, and V. I. Kolesnikov[1]

[1] *Rostov State Transport University, Rostov-on-Don, 344038 Russia*
[2] *Smart Materials Research Institute, Southern Federal University, Rostov-on-Don, 344090 Russia*
** e-mail: guda@sfedu.ru*

Received September 10, 2021; revised November 10, 2021; accepted November 18, 2021

Abstract—Mechanical and tribological properties of the steel surface can be improved by $Ti_xAl_{1-x}N$ multilayer coatings. Their rational design starts from a deep understanding of the functional relation of synthesis parameters, morphology, and crystallinity to final properties of layers. This problem can be described as experimentally intractable as it requires numerous specimens, spectroscopic characteristics, and tribological tests to cover a large multidimensional parameter space. The present paper discusses the possibility of predicting the mechanical and tribological properties of coatings by machine learning methods. The algorithm is trained on a set of theoretical micromechanical calculations. The quality of predictions is determined by comparing between several machine learning methods: ridge regression, random forest, radial basis functions, and neural networks. The machine learning approach is shown to be applicable to reverse engineering. The tandem neural network architecture is used to overcome the ambiguity problem and to predict Young's modulus and Poisson's ratio for each layer depending on the required mechanical parameters of the multilayer coating. The neural network topology is optimized so that the relative error comprises less than 5%.

Keywords: tribology, micromechanics, machine learning, neural networks, tandem architecture, reverse engineering

DOI: 10.1134/S1029959922040038

1. INTRODUCTION

The development of new engines, aircrafts, and high-speed trains poses new challenges in the design of heavily loaded friction units aimed to increase the service life and reduce tribological losses in tribocouples [1]. New generation coatings, called adaptive, are able to change their properties depending on the operating conditions. For example, Ti-Al-N films are adaptive to oxidation resistance. The protective properties of such coatings can be enhanced by introducing chromium, which ensures the thermal stability of the coating structure [2–4]. The tribological properties of the coatings are improved by optimizing the thickness, friction coefficient, and resistance to elastic and plastic deformation. The thickness of coatings on the contact surfaces of loaded friction pairs must be reduced in order to avoid the distortion of friction contact geometry and the formation of stresses in the coating during operation. Other mentioned parameters of nitride cermet coatings can be modified by introducing additional components during coating deposition, as well as by changing the coating architecture. For example, high friction wear resistance was shown for single-layer CrAlSiN coatings and those deposited in alternation with carbon precursors [5].

Progress in machine learning methods and big data analysis allows computational screening of new materials in order to select the required composition and morphology for specific tasks [6]. The open literature contains a large amount of data about the structure and properties of molecules and solid materials that can be used to train machine learning algorithms [7]. Of great interest is the screening of new materials based on structure–property–activity correlations [8]. In [9], a python-based molecular simulation design framework MoSDeF was applied to screen functionalized monolayer films with an emphasis on

their tribological efficiency. Machine learning algorithms can significantly reduce experimental and computational costs [10]. This is primarily because they can be used to reconstruct unknown nonlinear dependencies in experimental or observational data [11–13]. Starting with the works of Jones et al. [14], the use of artificial intelligence and neural networks in tribological applications has been constantly expanding in the last two decades [15], involving such diverse areas as wear of polymer composites [16, 17], tool wear [18], brake performance [19, 20], erosive wear of polymers [21], wheel and rail wear [22]. It is noteworthy that friction processes are affected by both microscopic material parameters (atomic binding energies, adhesion energy, defects and stresses in the crystal structure) and macroscopic parameters (surface morphology, coating thickness and strength, loading parameters, chemical reactions during tests). Machine learning methods speed up the testing of new materials by eliminating the need to repeat tedious calculations or experiments every time [23], which is particularly important for complex multicomponent systems.

Here we investigate the applicability of neural network algorithms for predicting the mechanical properties of a multilayer coating. Two options of algorithm application are considered. In a direct approach, coating properties are predicted based on the known parameters of each layer and the fraction of inclusions. In an inverse approach, the desired coating properties are achieved by finding one of the possible sets of parameter values for each layer and the fraction of inclusions.

2. METHODS

2.1. Mechanical Properties of the Multilayer Coating

The study is focused on exploring a TiAlN layered medium with alternating TiN and AlN layers. The multilayer coating model is shown in Fig. 1. The medium is transversely isotropic, with the x_3 transtropy axis perpendicular to the plane of the layers. The tensor of elastic constants of the layered medium $\mathbf{C}^{\text{eff}}$ is determined based on the differential scheme of the self-consistency method [24–27] for oblate spheroidal inclusions using the following relationship:

$$\frac{\mathrm{d}\mathbf{C}^{\text{eff}}(\varphi)}{\mathrm{d}\varphi}=\frac{1}{1-\varphi}\frac{\mathbf{C}_{\text{II}}-\mathbf{C}^{\text{eff}}(\varphi)}{\mathbf{E}+\mathbf{S}(\varphi)(\mathbf{C}_{\text{II}}-\mathbf{C}^{\text{eff}}(\varphi))/\mathbf{C}^{\text{eff}}(\varphi)}, \quad (1)$$

$$\mathbf{C}^{\text{eff}}(0)=\mathbf{C}_{\text{I}}(1),$$

where φ is the volume fraction of the material of inclusions in the medium, $\mathbf{S}$ is the Eshelby tensor for a transtropic medium, $\mathbf{E}$ is the unit tensor, and $\mathbf{C}_{\text{I}}$, $\mathbf{C}_{\text{II}}$ are the elastic constant tensors of the base and inclusion materials (isotropic materials). Note that using Eq. (1) the effective moduli of the layered medium can be calculated by simulating layers as infinitely thin disc-shaped lamellar inclusions [26, 27]. Such inclusions have the form of spheroids with semiaxes $a_1=a_2=a$, $a_3=\varsigma a$, where $\varsigma \ll 1$. The Eshelby tensor components are known in this case [28]. The effective elastic moduli of the layered medium were numerically calculated using the MATLAB software package. To verify the calculation results obtained with Eq. (1), the program was first tested for special cases for the Eshelby tensor components for an isotropic medium with spherical inclusions.

Such an approach to modeling the mechanical properties of ion-plasma sprayed coatings on the basis of their microstructural analysis was implemented in our previous works [26, 27]. There we presented the dependences of the elastic moduli of a homogeneous medium on the microstructural parameters of a multilayer coating. The results of modeling the effective elastic properties of the layered medium were quantitatively compared within micromechanical framework [26] and finite element approach [27]. In addition, the theoretical Young's modulus of the layered medium in the plane perpendicular to the spraying direction was compared with the results of a laboratory nanoindentation test on a TiAlN coating sample with a known Al/Ti ratio [29]. In [30], the Maxwell homogenization scheme was used to determine the effective properties of three types of 625 alloy coatings depending on microcracks and oxide inclusions.

2.2. Machine Learning Algorithms

The successful application of machine learning methods requires a sufficient collection of training data that would uniformly cover the space of values

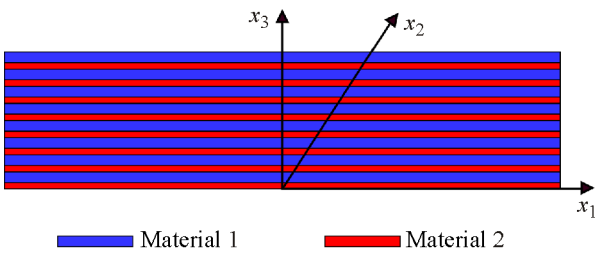

Fig. 1. Schematic view of a multilayer coating consisting of alternating layers of TiN (*1*) and AlN (*2*) (color online).

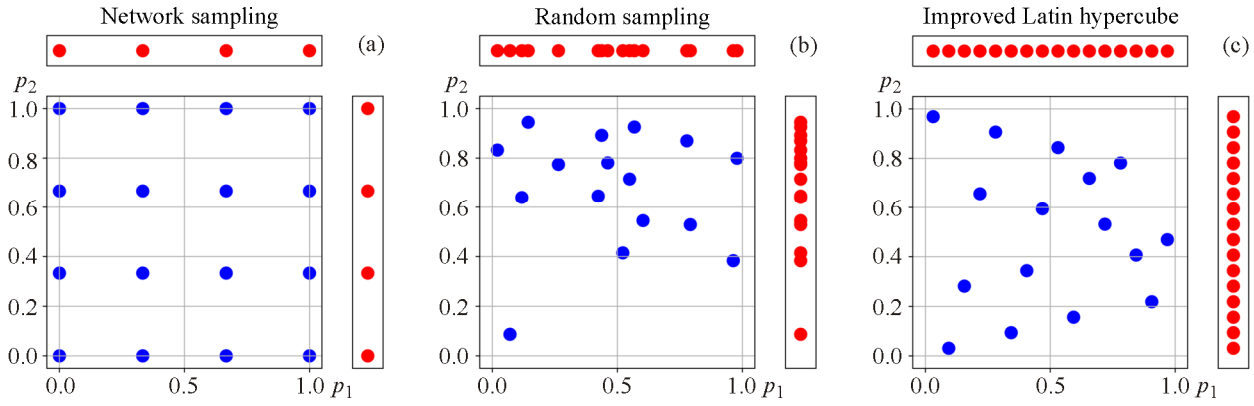

Fig. 2. Comparison of training sets generated by different methods: network (a), random (b), improved Latin hypercube sampling (c) (color online).

and the domain of the multivariate objective function. To predict the mechanical and tribological properties of coatings, we built a training set using the numerical solution of Eq. (1). The set was balanced by generating points in the parameter space with the improved Latin hypercube sampling (IHS) method. As an example, Fig. 2 shows the distributions of points in the training set consisting of 16 objects and their projections in the two-dimensional case.

The machine learning methods used were ridge regression, random forest, and neural network. Ridge regression is a linear regression that performs regularization to find optimal parameters. Let us consider a linear regression function that predicts the output $\hat{y}$ for each input vector $x=(x_1, x_1, ..., x_p)$ by the formula

$$\hat{y} = \omega_0 + \sum_{j=1}^{p} x_j \omega_j. \qquad (2)$$

The learning task for such a model is to find the optimal parameters $(\omega_j)_{j=1}^{p}$ for the objects of the training set $(x_i, y_i)_{i=1}^{N}$. The search for the optimal solution is carried out by the least squares method:

$$\mathrm{RSS}(\omega) = \sum_{i=1}^{N} (y_i - x_i^T \omega)^2 \to \min. \qquad (3)$$

The regression coefficients can grow significantly during learning, which seriously reduces the generalization ability of the method. To limit the growth of these coefficients, we added the Tikhonov regularization:

$$\mathrm{RSS}(\omega) = \sum_{i=1}^{N} (y_i - x_i^T \omega)^2 + \lambda \sum_{k=1}^{p} \omega_k^2 \to \min. \qquad (4)$$

The random forest algorithm [31] and a modified algorithm of extremely randomized trees (extra trees) [32] are ensemble algorithms, represented by a set of machine learning models (decision trees). The prediction of an ensemble algorithm in regression problems is performed by averaging the predictions of all models in the ensemble. For more stable ensemble predictions, each of the models included in the ensemble is trained not on the entire feature space, but on its randomly generated subset. Such subsets for each ensemble model are generated repeatedly.

Radial basis functions (RBF) in fact present an interpolation method. These are real functions $\varphi(x) = \varphi(\mathrm{v}x - c\mathrm{v})$ depending only on the distance to a center c. Using a linear combination of such functions, it is possible to approximate an unknown dependence in the training set data:

$$\hat{y}(x) = \sum_{i=1}^{N} \omega_i \varphi(\mathrm{v}x - x_i\mathrm{v}). \qquad (5)$$

The Euclidean norm is used as the norm for determining the radius, and a second-order polynomial is used as the radial function.

Artificial neural networks are a mathematical model of biological neural networks. In the general form, the response of an artificial neuron can be expressed by the equation

$$\sigma(x) = f\left(\omega_0 + \sum_{i=1}^{N} \omega_i x_i\right), \qquad (6)$$

where $f(x)$ is the neuron activation function. Here we used the following activation functions: sigmoid, hyperbolic tangent, and rectified linear unit (ReLU). Figure 3 illustrates the perceptron model used in this work. The input layer is a vector of input values of length n. The hidden layer consists of m neurons, each of which receives the same input signal at the input. The hidden layer can consist of several layers. The optimal architecture for the problems solved in this work was found to be a multilayer perceptron consisting of four hidden layers with 100, 200, 200,

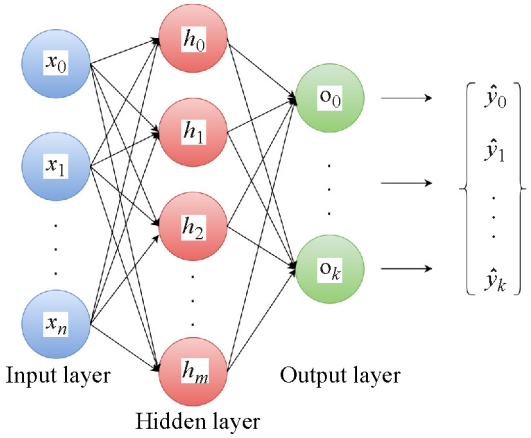

Fig. 3. Perceptron neural network used (color online).

and 100 neurons, respectively. The output layer consists of neurons that return the answer to the problem being solved. For the problem of classification into k classes, each of k output neurons predicts the probability of belonging to a certain class. For the regression problem, we use one neuron that returns a number.

When creating artificial neural networks, the weight coefficients ω are initialized in an arbitrary way. During learning, the weights in each layer are optimized using the iterative backpropagation algorithm [33]. At the first stage, the input signal is directly propagated through an artificial neural networks, i.e., the neural network prediction is computed for some input. Then, backpropagation begins. The calculation of partial derivatives during optimization requires that the activation function used be differentiable. In this work, we used the Adam weight optimization method [34].

As a rule, using the entire training set once to optimize the weights is not enough to get the best model. In this regard, the training set is mixed and fed to the input of artificial neural networks several times until the best quality of the algorithm is achieved. Each pass of the entire training set through artificial neural networks is usually called a training epoch.

The quality of the machine learning algorithm was evaluated as follows. Let there be a training set with objects $X=(x_1, x_2, ..., x_N)$ and answers $Y=(y_1, y_2, ..., y_N)$; the set $\hat{Y}=(\hat{y}_1, \hat{y}_2, ..., \hat{y}_N)$ presents artificial neural network predictions. The standard deviation function was used as a loss function in training artificial neural networks:

$$\mathrm{MSE}(X)=\frac{1}{N}\sum_{i=1}^{N}(y_i-\hat{y}_i)^2. \qquad (7)$$

The prediction quality of the machine learning model for the solved regression problem was assessed using the determination coefficient

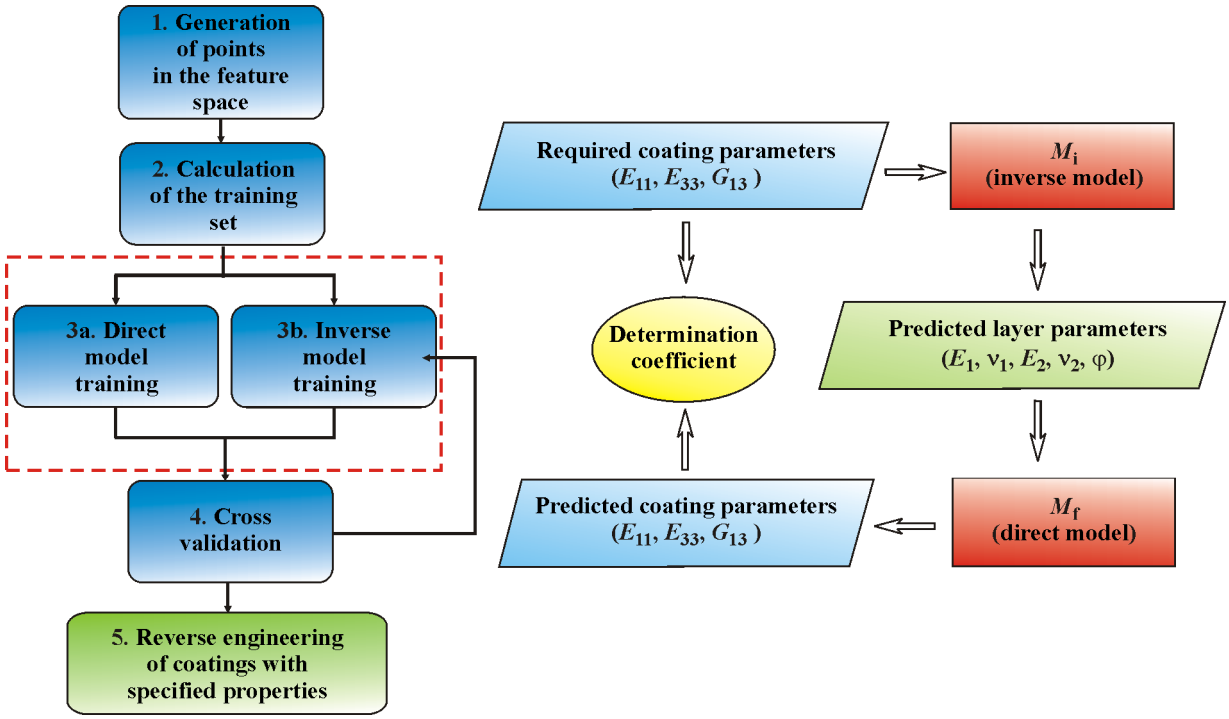

Fig. 4. Flow chart of applying machine learning methods for predicting the mechanical properties of the coating (a) and assessing the prediction quality of machine learning models (b) (color online).

Table 1. Results of comparing machine learning methods for direct problem solving

Training set size	Ridge regression	Radial basis functions	Extremely randomized trees	Multilayer perceptron
50	0.890	0.991	0.966	0.981
100	0.926	0.996	0.962	0.981
1000	0.979	0.999	0.992	0.999
10 000	0.976	0.999	0.998	0.999

$$R^2 = 1 - \frac{\sum_{i=1}^{N}(y_i - \hat{y}_i)^2}{\sum_{i=1}^{N}(y_i - \bar{y})^2}, \quad (8)$$

where

$$\bar{y} = \frac{1}{N}\sum_{i=1}^{N} y_i. \quad (9)$$

3. RESULTS

The general flow chart of the algorithms is shown in Fig. 4a. In the present work, two mutually inverse problems were solved.

1. Prediction of the effective mechanical properties of the layered medium, e.g., Young's moduli E_{11}, E_{33} and shear modulus G_{13} in a plane perpendicular to the x_1x_2 isotropy plane based on Eq. (1). The input data in this case were E_i and ν_i of isotropic materials 1, 2 constituting the multilayer coating, and the volume fraction of the material of inclusions φ in the layered composition.

2. Prediction of the mechanical properties of isotropic materials 1, 2 such as E_i, ν_i, and volume fraction φ on the basis of specified technical constants of the layered medium.

Machine learning algorithms were trained using a training set of the mechanical property values of the coating. The set was generated in the parameter space $(E_1, \nu_1, E_2, \nu_2, \varphi)$ by the IHS method and contained 10 000 points. The parameter values varied in the following ranges: $E_{1,2} = 180$–400 GPa, $\nu_{1,2} = 0.2$–0.4, $\varphi = 0$–89. The great difference between the values is due to different units of measurement of the parameters. This imbalance between the values of the features used to train machine learning models can lead to unstable behavior of the model, especially when applying methods that are sensitive to absolute feature values. In this regard, all input parameters were normalized so that their values were in the range from 0 to 1.

The mechanical properties of the layered medium were calculated for all points in space $(E_1, \nu_1, E_2, \nu_2, \varphi)$: Young's moduli E_{11}, E_{33} and shear modulus G_{13} in a plane perpendicular to the x_1x_2 isotropy plane. The resulting sets of points and the corresponding mechanical properties of the coating were used to train and test machine learning methods. The entire training set was divided into three parts in the ratio of 80% : 10% : 10%. The first part was used directly for the algorithm training. The second part was used for intermediate prediction quality control. The last part was a test set for checking the prediction quality of the trained model.

3.1. Comparison of Machine Learning Methods for Solving Direct and Inverse Problems

The first step was to solve a direct problem of predicting Young's moduli E_{11}, E_{33} and shear modulus G_{13} from the values of elastic moduli, Poisson's ratios, and the volume fractions of phases 1, 2 in the multilayer coating. The determination coefficient R^2 was used to assess the quality of predictions. Table 1 shows the prediction quality values of machine learning methods for training sets of different sizes. It can be seen from the table that the quadratic ridge regression method is the least accurate. The quality of predictions depends on the size of the training set, and saturation occurs when the number of points in a five-dimensional space is about 1000.

Since different sets of layer parameters can give the same mechanical properties of the coating, the inverse problem has a non-unique solution. In such a situation, machine learning methods are able to provide only one of the possible solutions, so the quality of predictions was assessed as follows:

– training of the machine learning model M_f to solve a direct problem, i.e., to predict (E_{11}, E_{33}, G_{13}) by the values of the parameters $(E_1, \nu_1, E_2, \nu_2, \varphi)$,

– training of the machine learning model M_i to solve an inverse problem, i.e., to predict the parameters $(E_1, \nu_1, E_2, \nu_2, \varphi)$ by given values of (E_{11}, E_{33}, G_{13}),

– assessment of the prediction accuracy of the model solving the inverse problem using the determi-

Table 2. Results of comparing machine learning methods for inverse problem solving

Training set size	Ridge regression	Radial basis functions	Extremely randomized trees	Multilayer perceptron
50	0.925	–144.548	0.981	0.906
100	0.963	–344.413	0.985	0.910
1000	0.997	–6854.715	0.993	0.957
10 000	0.997	–17011.606	0.997	0.999

nation coefficient R^2 calculated for the given values of (E_{11}, E_{33}, G_{13}) and the values predicted by the direct model M_f from the parameters predicted by the inverse model M_i. A schematic description of this approach is shown in Fig. 4b.

This approach to prediction quality assessment was based on the procedure for training tandem neural networks [35], which were used in the present work. Table 2 provides the values of the metrics R^2 for different machine learning methods that solve the inverse problem. All methods, except for RBF, provide a high accuracy solution. Radial basis functions as an interpolation method are unable to solve the inverse problem due to the ambiguity of the problem solutions, and therefore the predictions of such a model are random.

3.2. Optimization of the Tandem Neural Network Architecture

Ambiguity in the functional dependencies between the data prevents fast and reliable convergence to the optimal solution. This difficulty was overcome by using the tandem neural network architecture shown schematically in Fig. 5.

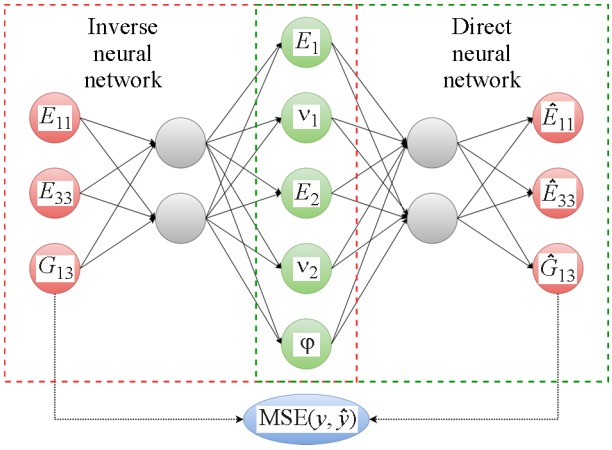

Fig. 5. Schematic diagram of operation and training of a tandem neural network (color online).

The tandem neural network consists of two parts: an inverse network and a direct network, each of which is trained separately. First, we trained the direct network, which returned the effective mechanical properties of the layered medium (E_{11}, E_{33}, G_{13}) using the set of parameters $(E_1, \nu_1, E_2, \nu_2, \varphi)$. Next, we trained the inverse network, which on the contrary returned the mechanical properties of isotropic materials and their volume fractions $(E_1, \nu_1, E_2, \nu_2, \varphi)$ according to the given mechanical properties of the layered medium. The output of the inverse network was connected to the input of the direct network, and the mean square error between the input values and the values obtained at the direct network output was used as a loss function. Thus, the intermediate layer connecting the two parts of the tandem network returns a set of parameters corresponding to the given properties of the layered medium. Due to the ambiguity of the parameters corresponding to the desired mechanical properties, the result obtained with the tandem network is one of the possible solutions.

A multilayer perceptron was used as both a direct and inverse neural network. The best result was obtained for networks with 4 hidden layers, which respectively contained 100, 200, 200, and 100 neurons. According to the input and target parameters of the direct and inverse problems, the input and output layer in the direct network consisted of 5 and 3 neu-

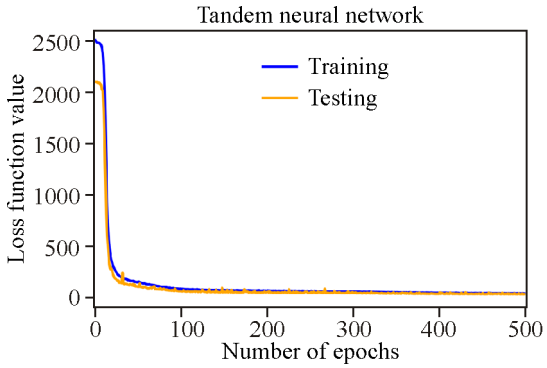

Fig. 6. Neural network error variation for the training and testing sets during training (color online).

Table 3. Relative error values for inverse problem solving by the tandem neural network method. Comparison of user-defined and numerically calculated (Eq. (1)) mechanical properties of the coating (E_{11}, E_{33}, G_{13}) based on the layer parameters (E_1, ν_1, E_2, ν_2, φ) predicted by the neural network

Desired coating parameter values (E_{11}, E_{33}, G_{13})	Layer parameters predicted by tandem neural network (E_1, ν_1, E_2, ν_2, φ)	Coating parameters (E_{11}, E_{33}, G_{13}) numerically calculated by Eq. (1) for layer parameters predicted by tandem neural network (E_1, ν_1, E_2, ν_2, φ)	Relative error, %
(200, 195, 75)	(192.50, 0.259, 349.21, 0.206, 29)	(198.77, 196.72, 78.35)	(0.61, 0.88, 4.46)
(248, 255, 90)	(236.41, 0.292, 397.95, 0.239, 39)	(248.02, 245.07, 95.13)	(0, 3.89, 5.70)
(308, 300, 117)	(292.31, 0.248, 399.90, 0.245, 51)	(305.20, 302.58, 121.6)	(0.91, 0.86, 3.93)
(355, 347, 135)	(340.60, 0.246, 400.00, 0.260, 62)	(350.86, 349.64, 140.2)	(1.16, 0.76, 3.85)
(387, 394, 144)	(378.74, 0.266, 400.00, 0.312, 75)	(384.07, 383.87, 150.2)	(0.75, 2.57, 4.30)

rons, respectively. In the inverse network, vice versa, there were 3 neurons for the input layer and 5 for the output one. An activation function in the direct network was ReLU, and in the inverse network it was a sigmoid function. Neural networks were trained over 500 epochs. The Adam optimizer with the learning rate parameter equal to 0.0001 was used as a network weight optimizer. Figure 6 shows the curves of variation in the magnitude of the neural network error during training.

The reliability of the solution obtained with the tandem neural network was assessed as follows. For given Young's moduli and shear modulus E_{11}, E_{33}, G_{13} of the multilayer coating (Fig. 1), the tandem neural network predicted the values of Young's moduli, Poisson's ratios, and the volume fraction of isotropic materials 1, 2 ($E_1, \nu_1, E_2, \nu_2, \varphi$). Then, we calculated the values of the layered medium parameters (E_{11}, E_{33}, G_{13}) for the obtained parameters ($E_1, \nu_1, E_2, \nu_2, \varphi$) of coating phases 1 and 2 using the numerical solution of Eq. (1). The relative error of the values was estimated by comparing the predicted values and the values obtained by the numerical solution of Eq. (1). Table 2 presents the error estimates for five sets of the mechanical property values of the layered medium. The average relative error for predicting the coating parameters does not exceed 3%, which indicates fairly high prediction accuracy.

4. DISCUSSION

It should be noted that for higher Young's and shear modulus values of $Ti_xAl_{1-x}N$ layered medium the tandem neural network also predicts higher parameters $E_1, \nu_1, E_2, \nu_2, \varphi$. The $Ti_xAl_{1-x}N$ multilayer coating, whose mechanical characteristics are given in the second row of Table 3, corresponds to the parameters predicted by the tandem neural network for TiN: $E_1 = 236.41$, $\nu_1 = 0.29$ and for AlN: $E_2 = 397.95$, $\nu_2 = 0.24$, with the Al/Ti ratio in weight percentage equal to 0.64. Multilayer coatings with 0.64 wt% Al/Ti ratio were studied in [30]. We made a comparison with the results of [30] where the authors give the values of reduced Young's modulus obtained by nanoindentation. The results obtained for the maximum indentation force (10 mN) were considered to exclude the influence of the mechanical characteristics of the substrate on the nanoindentation results. The reduced Young's modulus obtained by nanoindentation [30] was recalculated using the Oliver–Pharr model [36]. The relative error between the Young's modulus $E_{33} = 255$ GPa in the present study and the nanoindentation-based Young's modulus of the coating with the same Al/Ti ratio given in Table 1 in [30] did not exceed 5 and 10% for multilayer coatings with thick and thin layers, respectively.

The inverse problem cannot be solved with a software implementation of the numerical solution of Eq. (1) as it is impossible in this case to calculate gradients for using gradient descent optimization algorithms. This can be done by machine learning methods, especially artificial neural networks. The literature reports several examples of successful application of machine learning techniques to tribological problems. Regression models were used for tribological test results to predict the degree of wear for a copper surface modified with aluminum nitride and boron nitride particles [37]. The method of radial basis functions was applied to train the algorithm for predicting the friction coefficient of textured and porous surfaces [38]. Suitable descriptors were selected to describe the surface morphology. The quality of the algorithm depends on the completeness of training data. In [39], tool wear was predicted by a prognostic random forest method. The authors compared the performance of random forests with artificial

neural networks with feed forward back propagation and support vector regression.

Classical machine learning methods are unable to find the entire set of solutions in problems that have a nonunique solution. This paper proposes an approach for finding one of the possible solutions with high accuracy. Such problems can be effectively solved using the tandem neural network architecture. The problem of ambiguity of training set data is quite common, and there are several approaches to its solution. By introducing a new class for training set objects that cause ambiguity in data interpretation, it is possible to reduce the number of test set classification errors [40]. Another solution is to separate ambiguous objects from the training set [41]. For some pattern recognition problems, it is impossible to assign only one class label. More efficient training of convolutional neural networks for such problems is achieved by converting the label of each image into a discrete label distribution [42].

5. CONCLUSIONS

This paper considered the problem of optimizing the mechanical properties of a multilayer coating by selecting the properties of individual layers (Young's modulus, Poisson's ratio) and the volume fraction of the material of inclusions in the layered composition. A method was developed for solving the inverse problem of coating formation with given mechanical properties based on a tandem neural network. The architecture with the best prediction quality was composed of two identical multilayer perceptrons with four hidden layers consisting of 100, 200, 200, and 100 neurons. It was shown that a solution can be found when there are many ambiguous solutions, including continuous ambiguity. The quality of predictions estimated by the determination coefficient R^2 exceeds 0.99 for both the direct and inverse problems, provided the number of elements in the training set is more than 1000. The results obtained provide a basis for a digital technology of designing new tribological materials by machine learning to directly control the synthesis of materials. The use of this technology will permit the creation of functional materials with specified tribotechnical and mechanical characteristics for specific operating conditions.

FUNDING

This work was supported by the Russian Science Foundation (Project No. 21-79-30007).

REFERENCES

1. Meng, Y.G., Xu, J., Jin, Z.M., Prakash, B., and Hu, Y.Z., A Review of Recent Advances in Tribology, *Friction*, 2020, vol. 8, pp. 221–300. https://doi.org/10.1007/s40544-020-0367-2
2. Pfluger, E., Schroer, A., Voumard P., Donohue, L., and Munz, W.D., Influence of Incorporation of Cr and Y on the Wear Performance of TiAlN Coatings at Elevated Temperatures, *Surf. Coat. Technol*., 1999, vol. 115, pp. 17–23. https://doi.org/10.1016/s0257-8972(99)00059-6
3. Savan, A., Pfluger, E., Goller, R., and Gissler, W., Use of Nanoscaled Multilayer and Compound Films to Realize a Soft Lubrication Phase within a Hard, Wear-Resistant Matrix, *Surf. Coat. Technol*., 2000, vol. 126, pp. 159–165. https://doi.org/10.1016/s0257-8972(00)00542-9
4. Sousa, V.F.C., Da Silva, F.J.G., Pinto, G.F., Baptista, A., and Alexandre, R., Characteristics and Wear Mechanisms of TiAlN-Based Coatings for Machining Applications: A Comprehensive Review, *Metals*, 2021, vol. 11. https://doi.org/10.3390/met11020260
5. Kolesnikov, V.I., Vereskun, V.D., Kudryakov, O.V., Manturov, D.S., Popov, O.N., Novikov, E.S., Technologies for Improving the Wear Resistance of Heavily Loaded Tribosystems and Their Monitoring, *J. Frict. Wear*, 2020, vol. 41, pp. 169–173. https://doi.org/10.3103/s1068366620020051
6. Sun, S.J., Hartono, N.T.P., Ren, Z.K.D., Oviedo, F., Buscemi, A.M., Layurova, M., Chen, D.X., Ogunfunmi, T., Thapa, J., Ramasamy, S., Settens, C., DeCost, B.L., Kusne, A.G., Liu, Z., Tian, S., Peters, I.M., Correa-Baena, J.P., and Buonassisi, T., Accelerated Development of Perovskite-Inspired Materials via High-Throughput Synthesis and Machine-Diagnosis, *Joule*, 2019, vol. 3, pp. 1437–1451. https://doi.org/10.1016/j.joule.2019.05.014
7. Zhou, T., Song, Z., and Sundmacher, K., Big Data Creates New Opportunities for Materials Research: A Review on Methods and Applications of Machine Learning for Materials Design, *Engineering*, 2019, vol. 5, pp. 1017–1026. https://doi.org/10.1016/j.eng.2019.02.011
8. Masood, H., Toe, C.Y., Teoh, W.Y., Sethu, V., and Amal, R., Machine Learning for Accelerated Discovery of Solar Photocatalysts, *Acs Catalysis*, 2019, vol. 9, pp. 11774–11787. https://doi.org/10.1021/acscatal.9b02531
9. Summers, A.Z., Gilmer, J.B., Iacovella, C.R., Cummings, P.T., McCabe, C., MoSDeF, a Python Framework Enabling Large-Scale Computational Screening of Soft Matter: Application to Chemistry-Property Relationships in Lubricating Monolayer Films, *J. Chem. Theory Comput*., 2020, vol. 16, pp. 1779–1793. https://doi.org/10.1021/acs.jctc.9b01183
10. Saxena, S., Khan, T.S., Jalid, F., Ramteke, M., and Haider, M.A., In Silico High Throughput Screening of

Bimetallic and Single Atom Alloys Using Machine Learning and Ab Initio Microkinetic Modelling, *J. Mater. Chem. A*, 2020, vol. 8, pp. 107–123. https://doi.org/10.1039/c9ta07651d
11. Bucholz, E.W., Kong, C.S., Marchman, K.R., Sawyer, W.G., Phillpot, S.R., Sinnott, S.B., and Rajan, K., Data-Driven Model for Estimation of Friction Coefficient via Informatics Methods, *Tribol. Lett*., 2012, vol. 47, pp. 211–221. https://doi.org/10.1007/s11249-012-9975-y
12. Ali, Y., Rahman, R., and Raja, R., Acoustic Emission Signal Analysis and Artificial Intelligence Techniques in Machine Condition Monitoring and Fault Diagnosis: A Review, *J. Teknol*., 2014, vol. 69. https://doi.org/10.11113/jt.v69.3121
13. Liao, S.H., Chu, P.H., and Hsiao, P.Y., Data Mining Techniques and Applications—A Decade Review from 2000 to 2011, *Expert Syst. Appl*., 2012, vol. 39, pp. 11303–11311. https://doi.org/10.1016/j.eswa.2012.02.063
14. Jones, S.P., Jansen, R., and Fusaro, R.L., Preliminary Investigation of Neural Network Techniques to Predict Tribological Properties, *Tribol. Trans*., 1997, vol. 40, pp. 312–320. https://doi.org/10.1080/10402009708983660
15. Gandomi, A.H. and Roke, D.A., Assessment of Artificial Neural Network and Genetic Programming as Predictive Tools, *Adv. Eng. Software*, 2015, vol. 88, pp. 63–72. https://doi.org/10.1016/j.advengsoft.2015.05.007
16. El Kadi, H., Modeling the Mechanical Behavior of Fiber-Reinforced Polymeric Composite Materials Using Artificial Neural Networks—A Review, *Comp. Struct*., 2006, vol. 73, pp. 1–23. https://doi.org/10.1016/j.compstruct.2005.01.020
17. Jiang, Z.Y., Zhang, Z., and Friedrich, K., Prediction on Wear Properties of Polymer Composites with Artificial Neural Networks, *Comp. Sci. Tech*., 2007, vol. 67, pp. 168–176. https://doi.org/10.1016/j.compscitech.2006.07.026
18. Quiza, R., Figueira, L., and Davim, J.P., Comparing Statistical Models and Artificial Neural Networks on Predicting the Tool Wear in Hard Machining D2 AISI Steel, *Int. J. Adv. Manuf. Tech*., 2008, vol. 37, pp. 641–648. https://doi.org/10.1007/s00170-007-0999-7
19. Aleksendric, D. and Barton, D.C., Neural Network Prediction of Disc Brake Performance, *Tribol. Int*., 2009, vol. 42, pp. 1074–1080. https://doi.org/10.1016/j.triboint.2009.03.005
20. Bao, J.S., Tong, M.M., Zhu, Z.C., and Yin, Y., Intelligent Tribological Forecasting Model and System for Disc Brakem in *Proc. 24th Chinese Control and Decision Conference*, 2012, pp. 3870–3874. https://doi.org/10.1109/CCDC.2012.6243100
21. Zhang, Z., Barkoula, N.M., Karger-Kocsis, J., and Friedrich, K., Artificial Neural Network Predictions on Erosive Wear of Polymers, *Wear*, 2003, vol. 255, pp. 708–713. https://doi.org/10.1016/s0043-1648(03)00149-2
22. Shebani, A. and Iwnicki, S., Prediction of Wheel and Rail Wear under Different Contact Conditions Using Artificial Neural Networks, *Wear*, 2018, vol. 406, pp. 173–184. https://doi.org/10.1016/j.wear.2018.01.007
23. Tran, A., Furlan, J.M., Pagalthivarthi, K.V., Visintainer, R.J., Wildey, T., and Wang, Y., A Computationally Efficient Machine Learning Framework for Local Erosive Wear Predictions via Nodal Gaussian Processes, *Wear*, 2019, vol. 422, pp. 9–26. https://doi.org/10.1016/j.wear.2018.12.081
24. Giordano, S., Differential Schemes for the Elastic Characterization of Dispersions of Randomly Oriented Ellipsoids, *Eur. J. Mech. A. Solids*, 2003, vol. 22, pp. 885–902. https://doi.org/10.1016/S0997-7538(03)00091-3
25. Belyak, O.A. and Suvorova, T.V., Modeling Stress Deformed State upon Contact with the Bodies of Two-Phase Microstructure, *Solid State Phenomena*, 2020, vol. 299, pp. 124–129. https://doi.org/10.4028/www.scientific.net/SSpp.299.124
26. Kolesnikov, V.I., Suvorova, T.V., and Belyak, O.A., Modeling Mechanical Properties of Multilayer Coatings TiAlN, *Defect Diffus. Forum*, 2021, vol. 410, pp. 578–584. https://doi.org/10.4028/www.scientific.net/DDF.410.578
27. Kolesnikov, V.I., Suvorova, T.V., and Belyak, O.A., Mechanical Properties of Multilayer Coatings TiAlN, *J. Phys. Conf. Ser*., 2021, vol. 1954, p. 012019. https://doi.org/10.1088/1742-6596/1954/1/012019
28. Sevostianov, I., Yilmaz, N., Kushch, V., and Levin, V., Effective Elastic Properties of Matrix Composites with Transversely-Isotropic Phases, *Int. J. Solids Struct*., 2005, vol. 42, pp. 455–476. https://doi.org/10.1016/j.ijsolstr.2004.06.047
29. Kolesnikov, V.I., Kudryakov, O.V., Zabiyaka, I.Y., Novikov, E.S., and Manturov, D.S., Structural Aspects of Wear Resistance of Coatings Deposited by Physical Vapor Deposition, *Phys. Mesomech*., 2020, vol. 23, no. 6, pp. 570–583. https://doi.org/10.1134/s1029959920060132
30. Azarmi, F. and Sevostianov, I., Comparative Micromechanical Analysis of Alloy 625 Coatings Deposited by Air Plasma Spraying, Wire Arc Spraying, and Cold Spraying Technologies, *Mech. Mater*., 2020, vol. 144, pp. 103345. https://doi.org/10.1016/j.mechmat.2020.103345
31. Breiman, L., Random Forests, *Machine Learning*, 2001, vol. 45, pp. 5–32. https://doi.org/10.1023/a:1010933404324
32. Geurts, P., Ernst, D., and Wehenkel, L., Extremely Randomized Trees, *Machine Learning*, 2006, vol. 63, pp. 3–42. https://doi.org/10.1007/s10994-006-6226-1
33. David, E.R. and James, L.M., Learning Internal Representations by Error Propagation, in *Parallel Distributed Processing: Explorations in the Microstructure*

of Cognition: Foundations, MIT Press, 1987, pp. 318–362. https://doi.org/10.7551/mitpress/5236.001.0001

34. Kingma, D.P. and Ba, J., Adam: A Method for Stochastic Optimization, CoRR, abs/1412.6980, 2015. arXiv:1412.6980v9
35. Liu, D.J., Tan, Y.X., Khoram, E., and Yu, Z.F., Training Deep Neural Networks for the Inverse Design of Nanophotonic Structures, *Acs. Photonics*, 2018, vol. 5, pp. 1365–1369. https://doi.org/10.1021/acsphotonics.7b01377
36. Oliver, W.C. and Pharr, G.M., An Improved Technique for Determining Hardness and Elastic Modulus Using Load and Displacement Sensing Indentation Experiments, *J. Mater. Res*., 1992, vol. 7, pp. 1564–1583. https://doi.org/10.1557/jmr.1992.1564
37. Thankachan, T., Prakash, K.S., and Kamarthin, M., Optimizing the Tribological Behavior of Hybrid Copper Surface Composites Using Statistical and Machine Learning Techniques, *J. Tribol. Trans. ASME*, 2018, vol. 140. https://doi.org/10.1115/1.4038688
38. Boidi, G., da Silva, M.R., Profito, F.J., and Machado, I.F., Using Machine Learning Radial Basis Function (RBF) Method for Predicting Lubricated Friction on Textured and Porous Surfaces, *Surf. Topogr. Metrol. Prop*., 2020, vol. 8. https://doi.org/10.1088/2051-672X/abae13
39. Wu, D.Z., Jennings, C., Terpenny, J., Gao, R.X., and Kumara, S., A Comparative Study on Machine Learning Algorithms for Smart Manufacturing: Tool Wear Prediction Using Random Forests, *J. Manuf. Sci. Eng. Trans. ASME*, 2017, vol. 139. https://doi.org/10.1115/1.4036350
40. Trappenberg, T.P. and Back, A.D., A Classification Scheme for Applications with Ambiguous Data, in *Proc. IEEE-INNS-ENNS Int. Joint Conf. Neural Networks: IJCNN 2000*, Amari, S.I., Giles, C.L., Gori, M., and Piuri, V., Eds., 2000, vol. VI, pp. 296–301. https://doi.org/10.1109/ijcnn.2000.859412
41. Nalepa, J. and Kawulok, M., Selecting Training Sets for Support Vector Machines: A Review, *Artific. Int. Rev*., 2019, vol. 52, pp. 857–900. https://doi.org/10.1007/s10462-017-9611-1
42. Gao, B.B., Xing, C., Xie, C.W., Wu, J.X., and Geng, X., Deep Label Distribution Learning with Label Ambiguity, *IEEE Trans. Image Proc*., 2017, vol. 26, pp. 2825–2838. https://doi.org/10.1109/tip.2017.2689998